Polish Journal of Medical Physics and Engineering
The Journal of Polish Society of Medical Physics
ISSN 1898-0309, doi: 10.2478/pjmpe-2025-0011

June 2025
Vol 31, Issue 2

Scientific Paper

How to experimentally test the accuracy of quantitative SPECT images?

Hanna Piwowarska-Bilska [1,AD,*], Sara Kurkowska [1,BE], Jacek Iwanowski [1,BC], Małgorzata Poniatowska [1,D], Mateusz Piwowarski [2,CE], Bożena Birkenfeld [1,EF]

[1]Department of Nuclear Medicine, Pomeranian Medical University in Szczecin, Szczecin, Poland
[2]Department of Decision Support Methods and Cognitive Neuroscience, University of Szczecin, Szczecin, Poland
*Corresponding author: Hanna Piwowarska-Bilska; hanna.piwowarska@pum.edu.pl

(received 5 May 2024; revised 2 June 2024, 26 July 2024, 29 January 2025; accepted 14 February 2025)

Abstract

Introduction: Radiopharmaceutical therapy (RPT) uses radiopharmaceuticals that target cancer cells and is increasingly used as an oncological treatment. Estimating the absorbed dose of ionizing radiation in the patient's organs is the basis for personalized RPT. This article presents a technique for assessing the performance of a quantitative reconstruction using NEMA phantom. The goal of this work was to compare the accuracy of quantitative SPECT images using the same reconstruction algorithm but acquired with two different SPECT/CT systems from two different manufacturers.
Materials and Methods: We performed a series of SPECT/CT acquisitions of a NEMA IEC Body Phantom filled with ^{177}Lu using two gamma cameras. The images were reconstructed and quantified using Hermes software.
Results: There was no statistically significant difference in the results of recovered activities between the Symbia Intevo Bold and the NM/CT 850 gamma cameras. For a sphere with a diameter of 37 mm, the Rc values ranged from 0.69 to 0.75 for the Symbia Intevo Bold and 0.70 to 0.73 for the NM/CT 850. For a sphere with a diameter of 28 mm, the Rc values ranged from 0.61 to 0.71 for the Symbia Intevo Bold and 0.61 to 0.70 for the NM/CT 850. For a sphere with a diameter of 22 mm, the Rc values fell within the range of 0.56 to 0.63 for the Symbia Intevo Bold and 0.51 to 0.59 for the NM/CT 850.
Conclusions: Quantitative SPECT images are necessary to perform dosimetry calculations and before using them in the clinical settings it is important to perform validation. This validation can be simply performed by acquiring images of the phantom filled with known activity using the same acquisition and reconstruction parameters as those employed for patients studies. In our study we observed comparable performance between images acquired by the systems from two different manufacturers.

Introduction

Nuclear medicine allows diagnosis and treatment of patients using pharmaceutical products labelled with radioactive isotopes. In recent years, there has been a significant increase of hybrid tomographic scans: SPECT/CT (Single Photon Emission Computed Tomography/Computed Tomography) and PET/CT (Positron Emission Computed Tomography/Computed Tomography). Additionally, new radiopharmaceuticals are continually receiving regulatory approvals for both diagnostic and therapeutic purposes. Radiopharmaceutical therapy (RPT) is increasingly applied in the cancer treatment using radiopharmaceuticals that specifically target tumor tissue [1-5]. RPT can be an effective treatment, provided that the metastatic lesions receive an adequate dose of radiation, leading to their destruction. However, an increased absorbed dose (AD) in critical organs, such as for example bone marrow, kidneys, or salivary glands, can result in harmful side effects. Therefore, AD calculation has the potential to enable personalized RPT [6-9] and it can be performed using a post-therapeutic series of SPECT/CT images. The dosimetry workflow involves multiple steps (https://www.researchgate.net/figure/Clinical-dosimetric-workflow-scheme-Created-by-Manuel-Bardies-Used-with-his_fig20_344361284)[10], and it is crucial to ensure that the data created at the very beginning of the workflow is accurate; otherwise, systematic errors will propagate through the subsequent steps.

In recent years, two lutetium-177-labeled radiopharmaceuticals- ^{177}Lu-DOTATATE for neuroendocrine tumors (NET) and ^{177}Lu-PSMA-617 for prostate cancer, have been approved by the European Medicines Agency, U.S. Food and Drug Administration and Health Canada. In Poland, lutetium-177-labeled radiopharmaceuticals are already used in therapy, and we anticipate that many centers will soon be interested in introducing clinical internal dosimetry using 177Lu.

Authors' contribution: A – Research concept and design, B – Collection and/or assembly of data, C – Data analysis and interpretation, D – Writing the article, E – Critical revision of the article, F – Final approval of the article.

In this work, we aim to answer the question on how to assess the performance of a dosimetry system's quantitative reconstruction by using NEMA phantom. We compare the accuracy of quantitative SPECT images using the same reconstruction algorithm but acquired with two different SPECT/CT systems from two different manufacturers. We perform the measurements with ^{177}Lu, hoping that it will help other centers use our experience to guide their efforts into quantitative SPECT and dosimetry.

Materials and Methods

The work was performed at the Department of Nuclear Medicine of Pomeranian Medical University in Szczecin. The following devices were used:

1. Capintec CRC®-55t- Radioisotope Dose Calibrator.
2. Two gamma cameras: Symbia Intevo Bold from Siemens Healthineers and NM/CT850 from GE Healthcare.
3. Hermes Internal Dosimetry Software and workstation.

Calibration of the system with ^{177}Lu

For SPECT image quantification, the Hermes Internal Dosimetry program required the input of calibration factors (CF) for both gamma cameras.

Acquisitions were performed using a cylindrical homogeneous phantom filled with an aqueous solution of the radiopharmaceutical ^{177}Lu-DOTATAE, with an activity of 723.3 MBq.

Parameters of image acquisitions and reconstruction:

- Settings for both gamma cameras: energy windows TEW (Triple Energy Windows): the photopeak emission energy window 208 keV± 10% (187 keV-229 keV), lower- scatter (146 keV-187 keV), upper-scatter (229 keV-270 keV), matrix: 128x128.
- Acquisition protocol for Symbia Intevo Bold gamma camera: 90 projections, 30 s per projection, MELP collimator (medium energy low penetration); CT- standard low dose protocol.
- Acquisition protocol for NM/CT 850 gamma camera: 120 projections, 35 s per projection, MEGP collimator (medium energy general purpose); CT- standard low dose protocol.
- Reconstruction was performed with Hermes Internal Dosimetry software, using the ordered subset expectation maximization (OSEM) algorithm (4 iterations, 12 subsets) and a 3D Gaussian post-filter (cutoff frequency of 0.5 cycles/cm and an order of 10) with CT-based attenuation correction and Monte Carlo scatter correction (simulated photons: 10^6, update iterations: 2, down-scatter photons: 10^6).

The calibration factor was evaluated using the formula[11]:

$$CF\left[{}^{cps}\!/_{MBq}\right]=\frac{VOI\ total\ counts}{N\cdot t[s]\cdot A_c\left[MBq/cm^3\right]\cdot VOI\ volume\left[cm^3\right]} \quad (1)$$

where

VOI total counts – is the number of counts recorded inside a large Volume of Interest (VOI) drawn over the homogeneous activity area of the reconstructed phantom;
N – represents the number of SPECT projections;
t – is the projection time;
A_c – is the activity concentration in the phantom at the time of the scan; and
VOI volume – is the volume of the drawn VOI.

The determination of CFs for gamma cameras, based on the acquisitions of the cylindrical homogeneous phantom, was consulted and controlled by the Hermes service.

Testing the system using the NEMA IEC Body Phantom

The NEMA IEC Body Phantom (**Figure 1**) filled with an aqueous solution of ^{177}Lu-DOTATATE was used to simulate the patient.

The NEMA IEC Body Phantom contained 6 spheres with diameters: 37 mm, 28 mm, 22 mm, 17 mm, 13 mm, 10 mm. The activity concentration ratio of the spheres to the background was 6:1. The total activity in the phantom at the time of first acquisition was 660 MBq and the concentration of ^{177}Lu in the spheres was 0.41 MBq/ml. The Capintec meter accuracy for ^{177}Lu activity according to the current calibration certificate was 0.1%, with an expanded measurement uncertainty of 2.5%. The spheres were filled using a long needle intended for lumbar puncture. Activities in the syringe used for phantom filling were measured in the activity meter pre- and post-injections. The phantom was prepared by an experienced physicist under the supervision of

Figure 1. NEMA IEC Body Phantom.

a radiation protection officer. The following errors were avoided: isotope spill, air bubbles within the spheres or background.

The same two acquisition protocols previously used for the calibration phantom were applied to acquire the NEMA IEC Body Phantom. The acquisitions were performed over 5 working days using both gamma cameras. A total series of 10 SPECT/CT images were recorded for both gamma cameras. The time points for the GE NM/CT 850 were 4.62 h, 73.65 h, 105.48 h, 123.31 h and 141.37 h, while for the Symbia Intevo Bold: 3.48 h, 72.70 h, 106.20 h, 124.27 h and 142.30 h. The method used to reconstruct the NEMA IEC Body Phantom images on the Hermes workstation was the same as that described above for the cylindrical homogeneous phantom.

A series of acquisitions was performed to mimic the post-therapeutic imaging series done for patients undergoing RPT. These acquisitions were used in the subsequent validation of the dosimetry software workflow, including image registration, pharmacokinetic modeling (only the physical half-life was used for the phantom), time-integrated activity calculation, and the sphere model for AD calculation. In this paper, since the focus is on quantitative SPECT only, we use these acquisitions to evaluate the Rc values for different activities of the NEMA IEC Body Phantom.

The formula used in work of Gnesin et al.[12] was used to calculate the recovery coefficient (Rc) :

$$Rc = \frac{A_{SPECT}}{A_{ACTIVITY\ METER}} \quad (2)$$

where:

A_{SPECT} – the activity of the sphere measured on the SPECT image,

$A_{ACTIVITY\ METER}$ – the activity of the sphere measured with an activity meter, decay-corrected to the time of the scan.

A_{SPECT} was recovered from reconstructed images in units of Bq/ml.

The spheres were analyzed using spherical volumes of interest (VOIs) segmented on the CT images. Subsequently, these VOIs were transferred onto the co-registered reconstructed SPECT/CT images (**Figure 2, Figure 3**). As there was a non-zero background activity in the phantom, the recovery of that activity concentration was also calculated as a reference. Activity in the background was calculated as the mean of six sphere VOIs (each with a diameter of 40 mm) placed in the background (**Figure 3**).

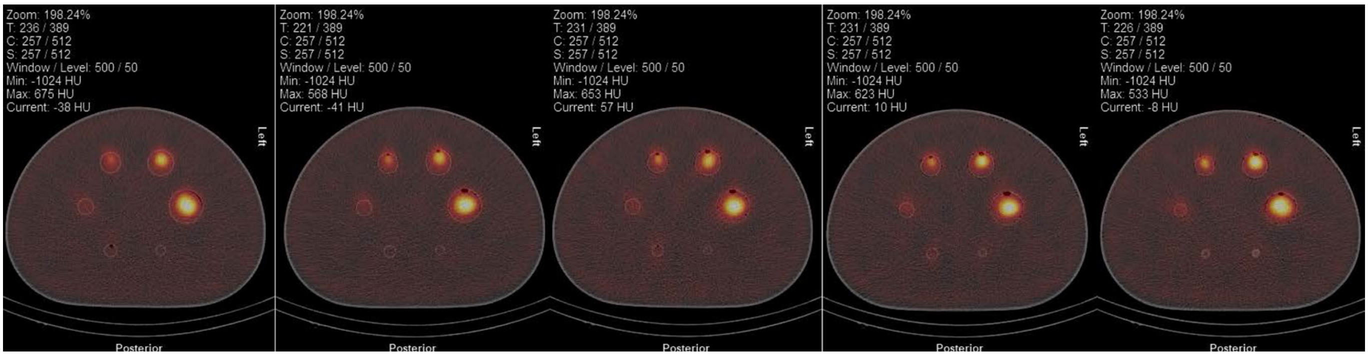

Figure 2. Cross sections of the NEMA IEC Body Phantom recorded 5 times with the Symbia Intevo Bold gamma camera, reconstructed and analyzed with Hermes software. VOIs for individual spheres are shown on the axial slice.

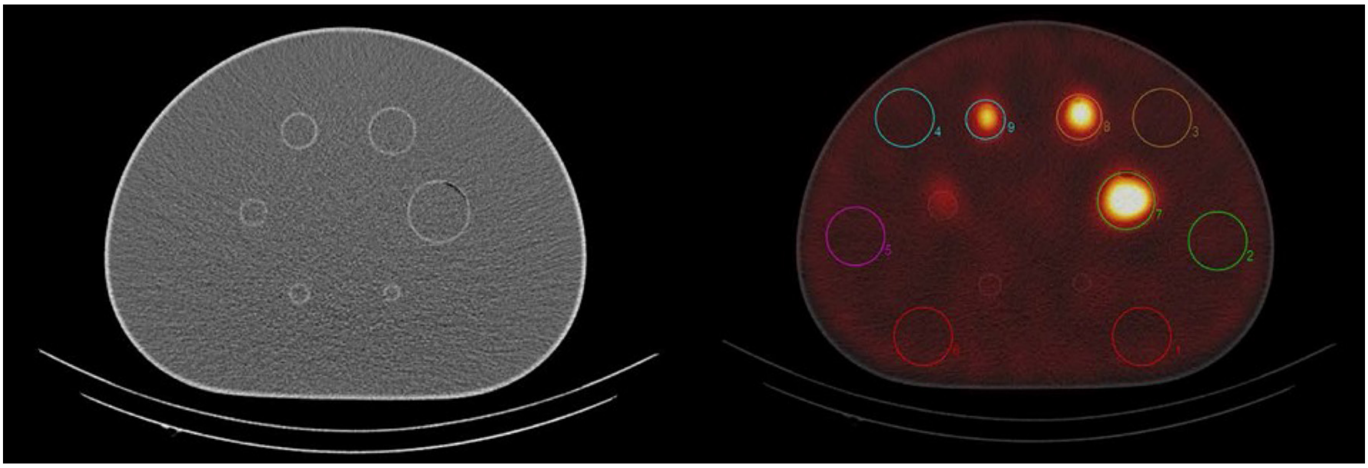

Figure 3. Cross sections of the NEMA IEC Body Phantom. On the left side: the CT image with the outline of hot spheres, on the right side: the SPECT/CT image. The VOIs for the hot spheres were determined based on the outlines of the spheres on the CT cross-section. In the SPECT/CT image, six identical background VOIs (numbered 1 to 6) were symmetrically placed in the peripheral part, while three VOIs (numbered 7 to 9) were positioned on the largest spheres located in the central part of the phantom.

We determined the Rc values for the three largest spheres and the background for different activities of the NEMA IEC Body Phantom acquired with two gamma cameras.

Additionally, the statistical significance of the differences in the measurement of the activities of the 3 largest spheres in the NEMA IEC Body Phantom acquired by two different gamma cameras was investigated. We used paired samples Wilcoxon's test using Statistica 13.1 software.

Moreover, we calculated the CFs for both gamma cameras using NEMA IEC Body Phantom acquisitions. The purpose of the calculations was to determine the variability of CF for different background activities in the phantom. The counts recorded in each of the six sphere VOIs placed in the background (**Figure 3**) was used for the calculations, as in the publication by Marin G. et al. from 2017 [13].

Results

The CFs for ^{177}Lu using a cylindrical homogeneous phantom were: for the Siemens Intevo Bold gamma camera: 10.6 cps/MBq, and for the NM/CT 850 gamma camera: 6.3 cps/MBq.

Table 1 shows the activity of the radiopharmaceutical in each sphere at the time of preparation of the NEMA IEC Body Phantom.

Table 1.Volumes, diameters and activities of the spheres in the NEMA IEC Body Phantom.

Sphere number	Sphere volume (ml)	Sphere diameter (mm)	Radiopharmaceutical activity calculated on measurement with an activity meter. (MBq)
1	26.5	37	10.9
2	11.5	28	4.7
3	5.6	22	2.3
4	2.6	17	1.1
5	1.2	13	0.5
6	0.5	10	0.2

Figure 2 shows an image from the Hermes program while performing activity recovery analysis of ^{177}Lu on selected cross-sections of the NEMA IEC Body Phantom recorded with a Symbia Intevo Bold gamma camera at 5 time points. The three smallest spheres were not included in the analysis due to their poor detection. **Figure 3** shows the method for VOIs placement for background and spheres activity estimation.

Figure 4 and **Figure 5** present the Rc values as a function of the total activity of the phantom for the acquisitions performed with the gamma camera Symbia Intevo Bold and GE NM/CT 850, respectively.

Table 2 presents the Rc values (ranges and averages) for the three spheres and the background in the NEMA IEC Body Phantom imaged with two gamma cameras.

Analysis of the differences in the measurement of the Rc of the 3 largest spheres acquired by two different gamma cameras showed that there was no statistically significant difference in the results of recovering the activity of gamma spheres with

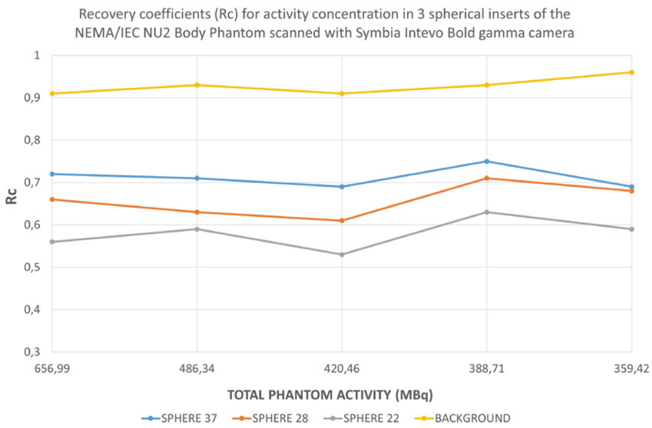

Figure 4. Recovery coefficient values for the 3 largest spheres and background in the NEMA IEC Body Phantom imaged with a Symbia Intevo Bold gamma camera.

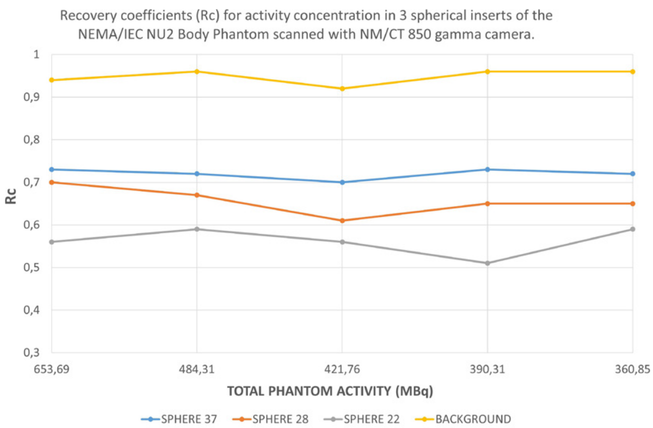

Figure 5. Recovery coefficient values for the 3 largest spheres and background in the NEMA IEC Body Phantom imaged with the NM/CT 850 gamma camera.

Table 2. Ranges and averages of Rc values for the three hot spheres and the background in the NEMA IEC Body phantom recorded for five different time points using two gamma cameras.

NEMA IEC Body Phantom	Symbia Intevo Bold		NM/CT 850	
VOI	Rc range	Rc mean ± sd	Rc range	Rc mean ± sd
Sphere Ø 37 mm	0.69–0.75	0.71±0.02	0.70–0.73	0.72±0.01
Sphere Ø 28 mm	0.61–0.71	0.66±0.04	0.61–0.70	0.66±0.03
Sphere Ø 22 mm	0.56–0.63	0.58±0.04	0.51–0.59	0.56±0.03
Background	0.91–0.96	0.93±0.02	0.92–0.96	0.95±0.02

the Symbia gamma camera and the NM/CT 850 gamma camera; $p=0.51$ at a significance level of $\alpha=0.05$.

Figure 6 shows the CFs as a function of the total activity of the NEMA IEC Body Phantom acquired using two gamma cameras. Each point on the graph represents the CF calculated for six spherical VOIs with a diameter of 40 mm, placed in the background in the peripheral part of the phantom, as shown in Figure 3. In Symbia Intevo Bold, the CF was in the range of 10.13-10.38, with an average of 10.25 ±0.10 and coefficient of variation of 1.01%. In NM/CT 850 the CF value was in the range of 5.39-5.59, with an average of 5.51 ±0.08 and coefficient of variation of 1.45%.

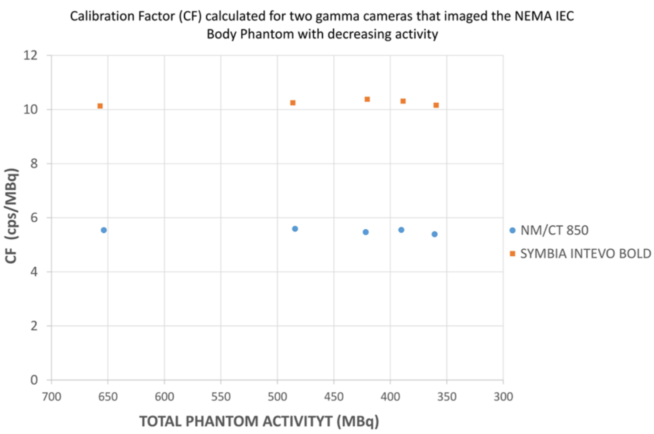

Figure 6. CF for ^{177}Lu calculated for NEMA IEC Body Phantom at 5 different time points, imaged using two gamma cameras. Each point on the graph represents the CF value calculated from six VOIs with a diameter of 4 cm, placed in the background in the peripheral part of the phantom, as shown in Figure 3.

Discussion

The total activity of ^{177}Lu used to fill the NEMA IEC Body Phantom varies in different studies [14-19]. In our study, we used a relatively low activity of ^{177}Lu, similar to the studies [18-19].

Activity recovery and therefore AD estimates for lesions less than 2 cm in diameter may be subject to significant error; hence, only the three largest spheres were analyzed in this study.

Based on the obtained Rc values, it can be concluded that both gamma cameras similarly recover the activity value of the ^{177}Lu for the three largest spheres of the NEMA phantom.

The results of Rc measurements for the ^{177}Lu obtained in this work correspond to those presented in other publications on phantom measurements performed under analogous conditions [18-19] in SPECT/CT studies. In a paper Tran-Gia et al. from 2019 [16], Rc coefficients were higher after using activity concentration ^{177}Lu in spheres 1.31 MBq/ml and Flash3D (with 48 iteration and 1 subset) image reconstruction technique. In a 2021 paper, Tran-Gia et al. [17]obtained Rc results for the largest sphere in the NEMA IEC Body Phantom between 0.7 and 0.9 for different gamma cameras. The higher recovery coefficient was obtained by using a longer acquisition time of 60 sec/projection. Such a long acquisition time is relatively rare for patients during clinical studies.

The low variability of the CF values for both gamma cameras, determined using the NEMA IEC Body Phantom with decreasing ^{177}Lu activity, indicates a relatively stable level of detector sensitivity in both devices for the tested activity range.

The calculated CF values for each camera using a NEMA IEC Body Phantom were lower than the results obtained using a homogeneous cylindrical phantom. It was shown [20-22] that the result of CF calculations is significantly affected by the chosen measurement technique. In a 2017 paper, Mezzenga E et al. [21] found gamma camera calibration performed with large homogeneous phantom to be optimal. Therefore, we used the obtained CFs with the NEMA phantom solely to assess the stability of gamma camera calibration results.

The lack of standardization of clinical internal dosimetry makes it difficult to compare measurements obtained at different nuclear medicine centers [23]. Different manufacturers of gamma cameras propose different methods of measuring detector sensitivity and different methods of image reconstruction. Having two gamma cameras from different manufacturers, the authors had trouble standardizing the acquisition protocol for phantom measurements. Programs for internal dosimetry also vary widely. There are dedicated programs, integrated with the gamma camera's manufacturer software. Some programs for internal dosimetry perform reconstruction of SPECT/CT and PET/CT images, while others require already reconstructed images. The authors of this paper believe that introducing standardization of internal dosimetry techniques could improve its quality and efficiency. Commercial dosimetry software generates a report of absorbed doses of ionizing radiation in individual organs and tissues of the patient. However, it is the user responsibility to ensure that the input data is correct and has physical meaning. Therefore, it is crucial to validate dosimetry systems to ensure the accurate assessment of the results of RPTs based on quantitative imaging of patients. In nuclear medicine departments that do not have the NEMA IEC Body Phantom, a cylinder of the commonly used Jaszczak phantom with attached bottles filled with radioisotope can be used for testing. It is also good practice to borrow phantoms from other facilities and have inter-center consultation of the calibration results of the equipment used.

Conclusions

1. Quantitative SPECT images are necessary to perform dosimetry calculations and before using them in the clinical settings it is important to perform validation. This validation can be simply performed by acquiring images of the phantom filled with known activity using the same acquisition and reconstruction parameters as those employed for patients studies.
2. In our study we observed comparable performance between images acquired by the systems from two different manufacturers.

References

1. Lepareur N, Ramee B, Mougin-Degraef M, Bourgeois M. Clinical Advances and Perspectives in Targeted Radionuclide Therapy. *Pharmaceutics.* 2023;15:1733. https://doi.org/10.3390/pharmaceutics15061733.
2. Shah HJ, Ruppell E, Bokhari R, Aland P, Lele VR, Ge C, McIntosh LJ. Current and upcoming radionuclide therapies in the direction of precision oncology: A narrative review. *Eur J Radiol Open.* 2023;31(10):100477. doi: 10.1016/j.ejro.2023.100477.

3. Sgouros G, Dewaraja YK, Escorcia F, Graves SA, Hope TA, Iravani A, et al. Tumor Response to Radiopharmaceutical Therapies: The Knowns and the Unknowns. *J Nucl Med*. 2021;62:12S-22S.
4. Piwowarska-Bilska H, Kurkowska S, Birkenfeld B. Individualization of Radionuclide Therapies: Challenges and Prospects. *Cancers*. 2022;14:3418. doi:10.3390/cancers14143418.
5. Echigo H, Mishiro K, Munekane M, Fuchigami T, Washiyama K, Takahashi K, et al. Development of probes for radiotheranostics with albumin binding moiety to increase the therapeutic effects of astatine-211 (211At). *Eur J Nucl Med Mol Imaging*. 2023. https://doi.org/10.1007/s00259-023-06457-0.
6. Huizing DMV, de Wit-van der Veen BJ, Verheij M, Stokkel MPM. Dosimetry methods and clinical applications in peptide receptor radionuclide therapy for neuroendocrine tumours: a literature review. *EJNMMI Res*. 2018;8(1):89. doi: 10.1186/s13550-018-0443-z.
7. Sjogreen Gleisner K, Chouin N, Gabina PM, Cicone F, Gnesin S, Stokke C, et al. EANM dosimetry committee recommendations for dosimetry of 177Lulabelled somatostatin-receptor- and PSMA-targeting ligands. *Eur. J. Nucl. Med. Mol. Imaging*. 2022;49:1778-1809.
8. Alipour R, Jackson P, Bressel M, Hogg A, Callahan J, Hicks RJ, et al. The relationship between tumour dosimetry, response, and overall survival in patients with unresectable Neuroendocrine Neoplasms (NEN) treated with 177Lu DOTATATE (LuTate). *Eur J Nucl Med Mol Imaging.* 2023;50(10):2997-3010. doi: 10.1007/s00259-023-06257-6.
9. O'Donoghue J, Zanzonico P, Humm J, Kesner A. Dosimetry in Radiopharmaceutical Therapy. *Journal of Nuclear Medicine.* 2022;63(10):1467-1474. doi: 10.2967/jnumed.121.262305.
10. Bardies M, Gear JI. Scientific Developments in Imaging and Dosimetry for Molecular Radiotherapy. *Clin Oncol (R Coll Radiol)*. 2021;33(2):117-124. doi: 10.1016/j.clon.2020.11.005.
11. Hermes Medical Solution. HybridViewer Dosimetry Handbook version 5.1 2020.
12. Gnesin S, Leite Ferreira P, Malterre J, Laub P, Prior JO, Verdun FR. Phantom Validation of Tc-99m Absolute Quantification in a SPECT/CT Commercial Device. *Comput Math Methods Med*. 2016;2016:4360371. doi: 10.1155/2016/4360371.
13. Marin, G., Vanderlinden, B., Karfis, I. et al. Accuracy and precision assessment for activity quantification in individualized dosimetry of 177Lu-DOTATATE therapy. *EJNMMI Phys.* 2017;4(1):7.
14. Staanum PF. Tumor dosimetry using 177Lu: influence of background activity, measurement method and reconstruction algorithm. *EJNMMI Phys*. 2023;10(1):39. doi: 10.1186/s40658-023-00561-8.
15. Huizing DMV, Sinaasappel M, Dekker MC, Stokkel MPM, de Wit-van der Veen BJ. 177 Lutetium SPECT/CT: Evaluation of collimator, photopeak and scatter correction. *J Appl Clin Med Phys*. 2020;21(9):272-277. doi: 10.1002/acm2.12991.
16. Tran-Gia Q J, Lassmann M. Characterization of Noise and Resolution for Quantitative 177Lu SPECT/CT with xSPECT. *Journal of Nuclear Medicine*. 2019;60(1):50-59. doi: 10.2967/jnumed.118.211094.
17. Tran-Gia J, Denis-Bacelar AM, Ferreira KM, Robinson AP, Calvert N, Fenwicket AJ, et al. A multicentre and multi-national evaluation of the accuracy of quantitative Lu-177 SPECT/CT imaging performed within the MRTDosimetry project. *EJNMMI Phys.* 2021;8:55. https://doi.org/10.1186/s40658-021-00397-0.
18. Di Domenico G, Di Biaso S, Longo L, et al. Validation of 99mTc and 177Lu quantification parameters for a Monte Carlo modelled gamma camera. *EJNMMI Phys.* 2023;10:27.
19. Peters SMB, Meyer Viol SL, van der Werf NR, de Jong N, van Velden FHP, Meeuwis A, Konijnenberg MW, Gotthardt M, de Jong HWAM, Segbers M. Variability in lutetium-177 SPECT quantification between different state-of-the-art SPECT/CT systems. *EJNMMI Phys*. 2020;7(1):9. doi: 10.1186/s40658-020-0278-3.
20. Zhao W, Esquinas PL, Hou X, Uribe CF, Gonzalez M, Beauregard JM, Dewaraja YK, Celler A. Determination of gamma camera calibration factors for quantitation of therapeutic radioisotopes. *EJNMMI Phys*. 2018;5(1):8. doi: 10.1186/s40658-018-0208-9.
21. Mezzenga E, D'Errico V, D'Arienzo M, Strigari L, Panagiota K, Matteucci F, Severi S, Paganelli G, Fenwick A, Bianchini D, Marcocci F, Sarnelli A. Quantitative accuracy of 177Lu SPECT imaging for molecular radiotherapy. *PLoS One*. 2017;12(8):e0182888. doi: 10.1371/journal.pone.0182888.
22. D'Arienzo M, Cazzato M, Cozzella ML, Cox M, D'Andrea M, Fazio A, Fenwick A, Iaccarino G, Johansson L, Strigari L, Ungania S, De Felice P. Gamma camera calibration and validation for quantitative SPECT imaging with (177)Lu. *Appl Radiat Isot*. 2016;112:156-164. doi: 10.1016/j. apradiso.2016.03.007.
23. Huizing DMV, Peters SMB, Versleijen MWJ, Martens E, Verheij M, Sinaasappel M, Stokkel MPM, de Wit-van der Veen BJ. A head-to-head comparison between two commercial software packages for hybrid dosimetry after peptide receptor radionuclide therapy. *EJNMMI Phys*. 2020;7(1):36. doi: 10.1186/s40658-020-00308-9.